Journal of Applied Polymer Science

Effect of a Chain Extender on the Properties of Poly(lactic acid)/Zinc Oxide/Copper Chlorophyll Acid Antibacterial Nanocomposites

Weihua Fan,[1,2] Yue Zhao,[2] Aijing Zhang,[2] Yukun Liu,[2] Yanxia Cao,[2] Jinzhou Chen[2]

[1]School of Nursing, Zhengzhou University, Zhengzhou 450001, People's Republic of China

[2]School of Materials Science and Engineering, Zhengzhou University, Zhengzhou 450001, People's Republic of China

Correspondence to: W. Fan (E-mail: fanweihua@zzu.edu.cn)

ABSTRACT: Poly(lactic acid) (PLA)/nano zinc oxide/copper chlorophyll acid (CCA) antibacterial nanocomposites with excellent mechanical properties were prepared in the presence of a chain extender named tolylene diisocyanate (TDI). The effect of the chain extender on the PLA long chain was confirmed by the increased molecular weight shown in the mass flow rate and gel permeation chromatography. *Escherichia coli* were adopted to examine the antibacterial ability of the blends. The effect of CCA is also discussed with regard to the enhancement of the antibacterial effect of zinc oxide (ZnO) over *E. coli*. Scanning electron microscopy and transmission electron microscopy were used to view the agglomeration and dispersion of ZnO in the PLA matrix. Differential scanning calorimetry and thermogravimetric analysis revealed a relatively stable thermal performance of the nanocomposites with and without TDI. A sharp increase in the mechanical properties was also observed after the addition of the chain extender under different processing conditions. Additionally, we found that the nanocomposites with the incorporation of TDI and the masterbatches in batches effectively improved the mechanical properties of PLA/ZnO/CCA without a sacrifice of the antibacterial effect. © 2014 Wiley Periodicals, Inc. J. Appl. Polym. Sci. **2015**, *132*, 41561.

KEYWORDS: composites; mechanical properties; morphology; nanoparticles; nanowires and nanocrystals; polyesters

Received 22 June 2014; accepted 24 September 2014

DOI: 10.1002/app.41561

INTRODUCTION

Biopolymers have received an increasingly essential attention in recent years for their biocompatibility and biodegradability. Among these, poly(lactic acid) (PLA) is the most promising candidate for packing end-use applications because of its renewability, high strength, and stiffness.[1–3] However, some issues, such as its insufficient toughness and low heat-distortion temperature, limit further application of PLA.[4] To overcome these drawbacks, copolymerization, blending, and filling techniques are normally used to improve the properties of PLA.[3] Nevertheless, blending has attracted more attention due to its economy and convenience in industrial production.

Nano zinc oxide, one kind of emerging multifunctional inorganic nanoparticle with photocatalytic and antibacterial activities, has been used as nanofillers for a lot of polymers to overcome their shortcomings.[5] It is well known for its high photocatalytic activity under UV light irradiation but not under sunlight.[6] As a result, some modification could be used to improve the activity under sunlight, enlarge the spectral response, and enhance the utilization of sunlight energies.[7,8] Copper chlorophyll acid (CCA) with a structure of the porphyrin rings is the main substance used to absorb and transmit light energy during photosynthesis. Because the top of the conduction band of zinc oxide (ZnO) is lower than the energy level of the first excited state of CCA, there may be an interface interaction between ZnO and CCA.[9,10] As a result, CCA was adopted to improve the photocatalytic efficiency and antibacterial activities of ZnO.

Our previous studies found that the addition of ZnO and CCA significantly improved the antibacterial activities of the nanocomposites. However, the mechanical properties were sharply reduced because of the degradation of PLA. It has been generally believed that the use of a chain extender could effectively increase the molecular weight and enhance the mechanical properties of polymers. Suitable chain extenders for polymers include bis(2-oxazoline)s, diisocyanates, bisepoxides, and polycarbodiimide, among which, the high reactivity of tolylene diisocyanate (TDI) has been studied and found to significantly enhance the molecular weight of PLA in a short time and under a low temperature.[11] Chen et al.[12] also found that the addition of methacryloyloxyethyl isocyanate (MOI) with the functional group isocyanate exhibited superior mechanical properties compared to PLA alone. Therefore, in our study, TDI was introduced to improve the mechanical properties of the nanocomposites.

Table I. Processing Conditions of the Samples

Sample	Composition	Procedure
P	PLA	PLA was extruded once.
P–T	PLA/1.5 wt %TDI	PLA and TDI were extruded simultaneously.
P–Z–C	PLA/1.2% ZnO/0.4% CCA	PLA and the antibacterial masterbatches were extruded simultaneously.
P–Z–C–T	PLA/1.2% ZnO/0.4% CCA/1.5%TDI	PLA, the antibacterial masterbatches, and TDI were extruded simultaneously.
2P–T–Z–C	PLA/1.2% ZnO/0.4% CCA/1.5%TDI	PLA and TDI were prepared in the first extrusion, and the antibacterial masterbatches was added in the second extrusion.
2P–Z–C–T	PLA/1.2% ZnO/0.4% CCA/1.5%TDI	PLA and the antibacterial masterbatches were prepared in the first extrusion, and TDI was added in the second extrusion.

The main objective of this study was to provide a simple but effective way to improve the mechanical properties of PLA/ZnO/CCA without any sacrifice of the antibacterial effect. The effects of the chain extender on the properties of the blends in different processing conditions during melt mixing were investigated. The antibacterial activities, morphology, thermal properties, and mechanical properties of the PLA/ZnO/CCA/TDI blends were also examined.

EXPERIMENTAL

Materials

The PLA used in this study was supplied by Kunshan HeZhi Plastic Technology Co., Ltd. (Suzhou, China). The selected grade, PLA 4032D, was a semicrystalline material in pellet form. Nano-ZnO was purchased by Aladdin Chemistry Co., Ltd. (Shanghai, China). The purity was 99.9%, and the particle size was 30 ± 10 nm. The sodium copper chlorophyllin was supplied by Zhengzhou Renren Chemical Products Co., Ltd. (Zhengzhou, China). TDI used as a chain extender was supplied by Sinopharm Chemical Reagent Co., Ltd.

Antibacterial Nanocomposite Preparation

Preparation of CCA. Hydrochloric acid was used to acidize the sodium copper chlorophyllin (SCC) to improve the compatibility with the matrix. An amount of 3 g of SCC was dissolved in 900 mL of distilled H_2O in the presence of 1 mL of hydrochloric acid in a 1-L round-bottom flask, and to dissolve it well, several minutes of mechanical stirring was necessary. CCA was finally achieved by vacuum suction filtration.

Antibacterial Masterbatches Preparation. Because of the small particle size, high surface energy, and strong polarity of ZnO make it difficult to disperse evenly in the matrix, the method of solution blending was used to reduce the agglomeration.

The mixture of ZnO and CCA were initially carried out by ultrasound for 2 h in chloroform and then blended with parts of dried poly(lactic acid) (P) together by mechanical stirring for 3 h. The antibacterial masterbatches were finally obtained by precipitation and vacuum suction filtration until the chloroform in the mixed solution was evaporated.

Antibacterial Nanocomposite Preparation. At first, PLA and ZnO were dried at 70°C for 24 h, and CCA was dried at 55°C for 24 h. To prepare the antibacterial nanocomposites, the antibacterial masterbatches and the rest of PLA were evenly mixed together (P–Z–C) in an RHR-10A high-speed mixer. The blends were then extruded by a corotating twin-screw extruder from Chemical Machinery Research Institute. The operating temperatures of the extruder were set at 155, 165, 175, 170, 175, 170, and 170°C (for the different zones from hopper to die). For the sake of comparison, P and poly(lactic acid) containing only 1.5% toluene diisocyanate (P–T) were processed under conditions similar to those discussed previously.

The sample of P–Z–C–T was adopted to examine the effect of the chain extender on the mechanical properties. The 2P–T–Z–C and 2P–Z–C–T samples (Table I) were prepared to investigate the effects of the processing times and processing sequences on the mechanical properties. The use of TDI was done according to our previous study in which 1.5% TDI was found to achieve the best mechanical properties. The specific strategies applied previously are summarized in Table I. After each extruding process, the composites were stretched into stripes in cold water after they emerged from the extrusion die and then pelletized and dried in an air-circulating oven at 55°C for at least 24 h.

To characterize the antibacterial activities, films with a thickness of about 0.5 mm and an area of 4×4 cm^2 were obtained by the molding of the dried composites pellets on a plate vulcanizing machine (the type was $600 \times 600 \times 2$ of Qingdao Yaxing Machinery Co., Ltd.).

Antibacterial Effect

To characterize the antibacterial effect of the P–Z–C–T blends, *Escherichia coli* was used according to ISO 22196-2007. *E. coli* were inoculated in the Luria–Bertani culture (1 g of trypton/0.5 g of yeast extract/0.5 g of NaCl/100 mL of distilled H_2O) and incubated in an orbital shaker rotated at 50 rpm at 37°C for 24 h under aerobic conditions. To ensure the quality of the bacteria, the process was repeated twice. Subsequently, the bacteria was inoculated on the surface of the composite films in the plate and covered with a PE film cut into 3×3 cm^2 square

Table II. Antibacterial Activities of the Samples

Sample	Average colony-forming units ($\times 10^6$ cfu/piece)	Antibacterial efficiency (%)
Colonies	4.564	0
P	3.843	15.8
P-T	3.362	26.3
P-Z-C	0.006	99.8
P-Z-C-T	0.029	99.4
2P-T-Z-C	0.037	99.2
2P-Z-C-T	0.045	99.0

pieces to prevent moisture from evaporating too fast and killing the bacteria. The plates were incubated in visible light at 37°C for 24 h. Finally, the bacteria cultivated well were diluted 10^3 times by elution (0.8 g of NaCl/100 mL of distilled H_2O) and transferred to a solid medium (2 g of agar/1 g of trypton/0.5 g of yeast extract/0.5 g of NaCl/100 mL of distilled H_2O). The solid medium containing bacteria was cultivated for at least 24 h in the incubator. The colony counts (cfu/piece) were calculated by multiplication of the number of colonies on the solid medium after 24 h of incubation by its dilution ratio. The antibacterial rate (R) was obtained by the calculation of the amount of the bacteria:

$$R(\%) = 100(B - C)/B$$

where B is the colony count of the bacteria (cfu/piece) and C is to the colony count of the sample.

Melt Mass Flow Rate (MFR)

MFR calculations were performed with a melt flow indexer (RL-5 of Shanghai Sierda Scientific Instrument Co., Ltd.). The execution standard was ISO 1133-1997, the temperature was set at 190°C, and the weight was 1835 g.

Gel Permeation Chromatography (GPC)

The molecular weight of the nanocomposites was determined by four Waters Styragel columns (HT 2, HT 3, HT 4, and HT 5), a Waters 1515 isocratic HPLC pump, and a Waters 2414 RI detector. The blends were first dissolved in chloroform and then mixed with THF. Polystyrene standards were used for the calibration.

Differential Scanning Calorimetry (DSC)

DSC tests were conducted by PerkinElmer Pyris Diamond DSC under a nitrogen atmosphere. The samples about 3–7 mg were cut off from the pellets, which were dried for at least 12 h at 50°C. The samples were heated at a rate of 10°C/min from 30 to 200°C, held at that temperature for 1 min, and then cooled to 30°C before a second heating scan from 30 to 200°C at a rate of 5°C/min.

Thermogravimetric Analysis (TGA)

TGA was used to test the thermal stability of the polymeric system in a certain temperature region. The 3–5-mg pelletized samples were dried in an air-circulating oven at 55°C for at least 24 h. The initial operating temperature was 30°C, and the final temperature was 420°C. The heating rate was 10°C/min. TGA and derivative thermogravimetry (DTG) were observed in the study.

Transmission Electron Microscopy (TEM)

TEM of Tecnai G^2 20 S-TWIN of FEI Co. was used at an accelerator voltage of 200 kV. The samples, with a thickness of about 50–100 nm, were cut by ultramicrotome at room temperature.

Scanning Electron Microscopy (SEM)

SEM was used to characterize the phase morphology of the samples by JEM-7500F from JEOL Co. (Japan). The samples were obtained from the cross section of the specimen in the tensile test.

Mechanical Properties

The mechanical properties consist of the tensile properties, impact properties, and bending properties. The dumbbell-shaped specimens were obtained by injection with dimensions of 172 mm in length, 10 mm in width, and 4 mm in thickness of the parallel portion according to ISO 527-2-1993. The tensile test was done with a CMT 5104 instrument of Shenzhen SANS Co., Ltd., at a speed of 20 mm/min. The dimensions of the bending tests were 80.0 × 10.0 × 4.0 mm^3 (Length × Width × Thickness). Meanwhile, the speed of the test was 2 mm/min. The Izod impact tests were measured according to ISO 179-1-2001 by a XJU-22 machine from Chengde Testing Machine Factory. All of the values were obtained at room temperature by the averaging of over seven specimens for each processing condition.

RESULTS AND DISCUSSION

Antibacterial Activities

The antibacterial activities of the different composite films were measured by a conventional plate count method.[13] An antibacterial plastic was reported to have a strong antibacterial effect only in the condition in which its R reached up to 99%, whereas when R reached up to 90%, it was reported to have an antibacterial effect according to the international standard of antimicrobial plastics shown previously.

As explained in Table II and Figure 1, no noticeable reduction in the *E. coli* colony was observed in the PLA film compared with the pure colony; this indicated that PLA had no antibacterial effect on *E. coli*. The result was same as that after the addition of TDI.

However, an obvious reduction in the colonies was observed in the nanocomposites containing ZnO/CCA. The antibacterial mechanism of the nanocomposites was mainly attributed to the ability of ZnO to catalyze the photooxidation of polymers. Specifically, the quantity of reactive oxygen species (ROS; ·OH, $^1O_2$, $O_2^{\cdot -}$) production in the course of photocatalysis determines the antibacterial effect.[14] After illumination, ZnO absorbs photons with energy equal or higher than its band gap energy. It leads to the formation of electron-hole pairs in which an electron is excited to the conduction band; this leaves a positive hole in the valence band. The electron can reduce molecular oxygen to superoxide anions ($O_2^{\cdot -}$s), which can be transformed to singlet oxygens ($^1O_2$s). The hole can oxidize water and hydroxyl to hydroxyl radicals (·OHs). The three types of ROSs

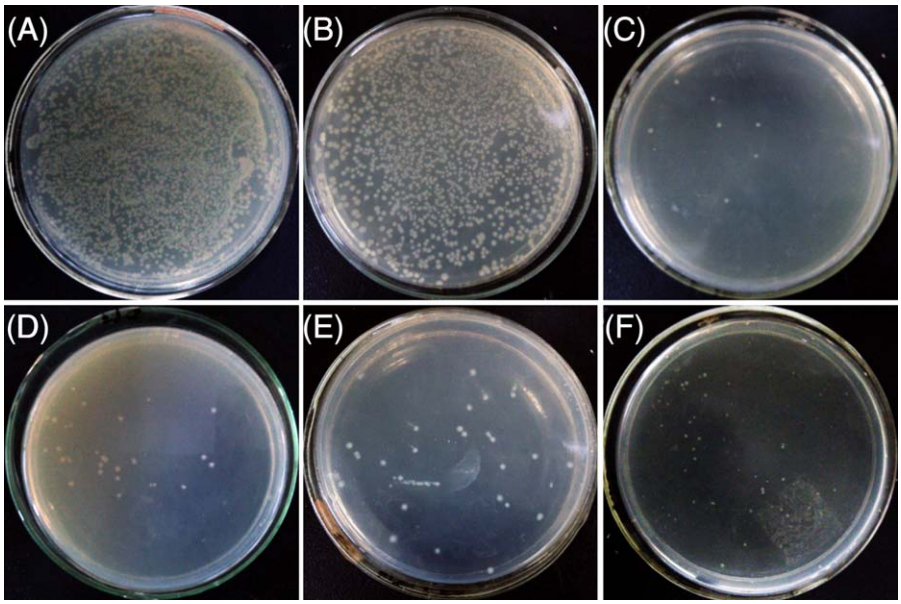

Figure 1. Antibacterial activity of (A) P, (B) P–T, (C) P–Z–C, (D) P–Z–C–T, (E) 2P–Z–C–T, and (F) 2P–T–Z–C. [Color figure can be viewed in the online issue, which is available at wileyonlinelibrary.com.]

may simultaneously contribute to antibacterial action.[15] Although the wide band gap of ZnO makes it require more energy to excite the electrons, CCA containing porphyrin rings with two conjugated double bonds can absorb and transmit light energy during photosynthesis. Because the top of the conduction band of ZnO was lower than the energy level of the first excited states of CCA, there were some interactions between ZnO and CCA.[9] It was confirmed by Fourier transform infrared and ultraviolet–visible spectroscopy in our previous studies,[16] in which we reported that the interaction made the visible region absorption of ZnO/CCA broader. According to Figure 1(3), the composite film of P–Z–C showed a strong antibacterial effect of up to 99.8% against *E. coli* with only 75.7% PLA/ZnO under the same conditions as used in our previous study.[16]

A slight reduction of *R* was observed after the addition of TDI, as shown in Figure 1(4). It was reasonably attributable to the incorporation of TDI; this decreased the number of the surface hydroxyl of ZnO. This led to a decrease in the photocarrier (electron-hole pairs) separation efficiency and an increase in the recombination probability of electrons and holes.[17] The changes

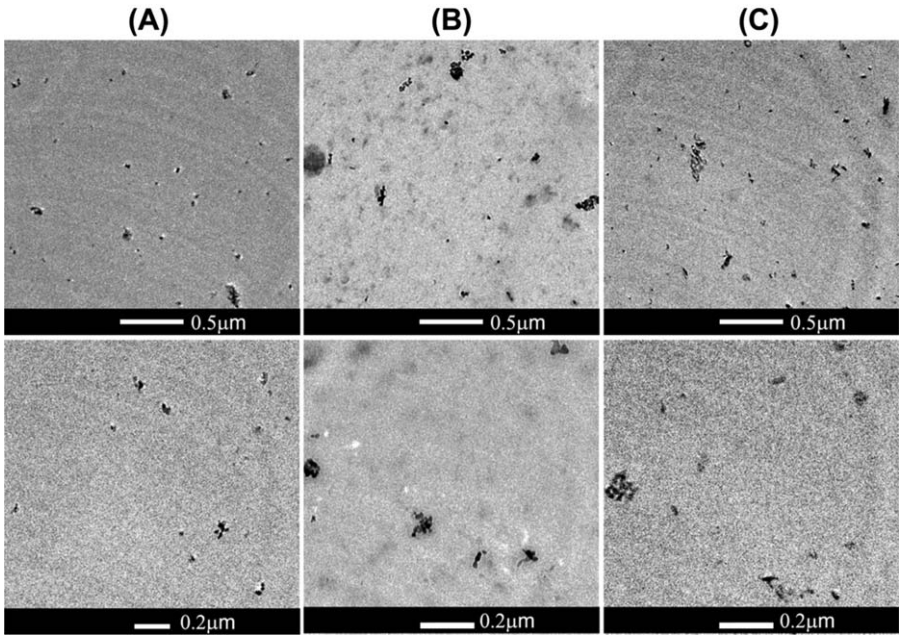

Figure 2. TEM micrographs of (A) P–Z–C, (B) P–Z–C–T, and (C) 2P–Z–C–T.

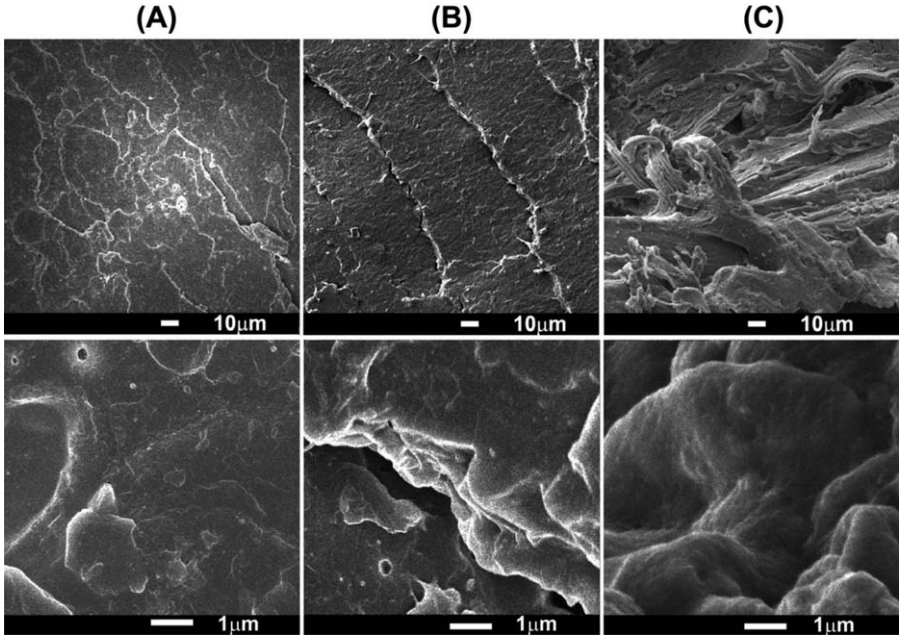

Figure 3. SEM micrographs of (A) P–Z–C, (B) P–Z–C–T, and (C) 2P–Z–C–T.

slightly decreased the ROS generation concentration and decreased the antibacterial activities.

Morphology

TEM micrographs of the blends with and without TDI with different incorporation methods are shown in Figure 2. The dark spots represent ZnO particles, and the gray areas corresponded to the PLA matrix. CCA could not be seen from the micrographs because of its low molecular weight.[18] The TEM images were measured at different magnifications, which characterized the distribution and the degree of ZnO aggregation in the PLA matrix. Obviously, the blends without TDI revealed a fairly uniform distribution and less aggregation. However, when TDI and the masterbatches were incorporated simultaneously to the PLA matrix, ZnO dispersion became deteriorated, and the aggregation was aggravated. This phenomenon was mainly attributed to competing effects.[3] The isocyanate groups of the chain extender could react with both the hydroxyl groups of the PLA and the hydroxyl groups on the surface of ZnO. This led to the poor dispersion of ZnO in the PLA matrix.[19] Meanwhile, when PLA and TDI were blended first, the excessive addition of TDI were consumed by not only the hydroxyl end groups but also by the carboxyl end groups of PLA.[11] Consequently, no more reactions were carried out between the PLA chains and ZnO particles; also, the reaction between PLA and excessive TDI further decreased the mechanical properties through the formation of crosslinking and a branch structure.[19] To improve the distribution of ZnO and reduce the degree of ZnO aggregation, a hypothesis is proposed that parts of carboxyl end groups of PLA were bonded with the hydroxyl groups of ZnO by the ester group[5] at first; then, the remaining hydroxyl groups of PLA reacted with TDI.[11] This decreased the agglomeration degree of ZnO and enhanced the compatibility between ZnO and PLA.[20,21] This exactly conformed to the results of the incorporation of TDI and the masterbatches in batches, as shown in Figure 2(C). Nevertheless, further analysis was needed to determine the specific reason.

Figure 3 shows the fractured cross sections of P–Z–C without and with TDI with different incorporated methods after stretching. The micrographs of the nanocomposites without TDI revealed a fairly smooth fracture surface of the dispersion phase with brittle deformation in Figure 3(A). This indicated bad interfacial interaction between the PLA matrix and ZnO. Interfacial debonding without perceptible plastic deformation[22] was observed, as shown in Figure 3(B); this led to the formation of worse interfacial interaction. When TDI and the masterbatches were added to the blends in batches, the plastic deformation of the PLA matrix was clearly observed, as shown in Figure 3(C).

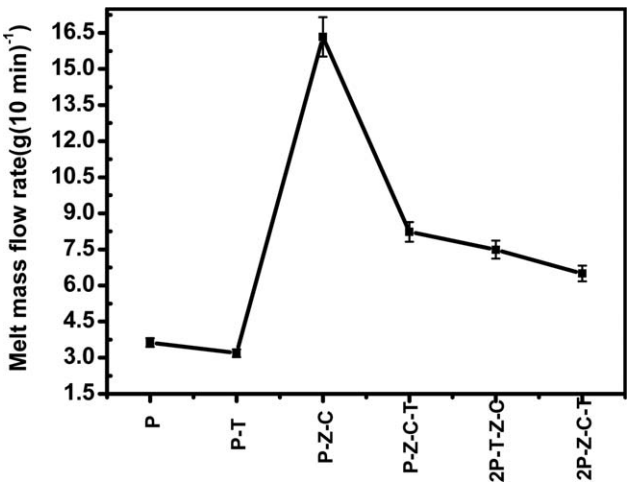

Figure 4. MFR results of the P, P–T, and blends. The test temperature was 190°C.

Table III. Molecular Weight Analyses of the Samples by GPC

Sample	Number-average molecular weight (Da)	Weight-average molecular weight (Da)	Polydispersity
P	130,797	201,009	1.537
P-T	133,280	218,480	1.639
P-Z-C	102,916	164,477	1.598
P-Z-C-T	109,441	175,329	1.602
2P-T-Z-C	111,486	175,718	1.548
2P-Z-C-T	107,141	170,149	1.514

As shown, small black cavities and crazes appeared, and the stress whitening layers were larger. This indicated the formation of better interfacial interaction between the PLA matrix and ZnO. In the course of stretching, aggregates of ZnO may have acted as sites of local stress concentration; these sites were capable of triggering cavities and crazes and released the strain constraint and led to the relaxation of the stress concentration.[23,24] This increased the toughness of the blends [Figure 3(C)]. On the contrary, when the crazes were not constrained by the interfacial effects, a rapid growth of cracks appeared and finally developed to crack fractures [Figure 3(B)]. This explanation was consistent with the mechanical properties of the nanocomposites.

Mechanical Properties

It is well known that one of the limitations of PLA toward wider industrial applications is its thermal and mechanical degradation during processing.[25] The degradation from PLA composites should be responsible for the reduction of its mechanical properties. Bitinis[23] evaluated the degradation of PLA by viscosity measurements and found a viscosity decrease of nearly four times and a reduction of the molecular weight of about 30% due to the chain scission process at 160°C for 15 min. Similar results were also found by other authors.[26] To evaluate the influence of the thermal degradation and mechanical degradation on the mechanical properties of PLA, MFR and GPC were adopted, and the results are shown in Figure 4 and Table III, respectively. Low MFR values indicated a higher viscosity value, higher molecular weight, and less degradation during the process.[27] The MFR values of the blends with and without TDI were investigated as follows.

As shown in Figure 4 and Table III, the MFR values of the PLA decreased slightly after the incorporation of 1.5% TDI; this indicated an increase in the viscosity values and a reduction of degradation. Although the MFR value of P–Z–C was up to 16.3 g (10 min)$^{-1}$; this indicated an obvious viscosity decrease of almost 3.5 times and a reduction in the molecular weight of

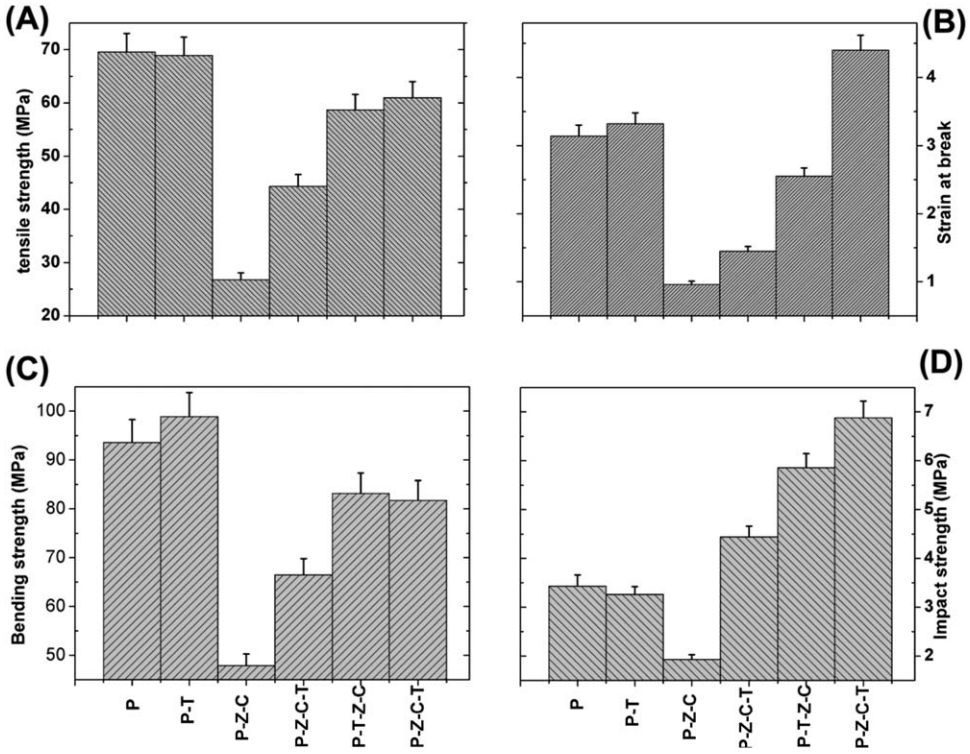

Figure 5. Mechanical properties of the P, P–T, and blends: (A) tensile strength, (B) strain at break, (C) bending strength, and (D) impact strength.

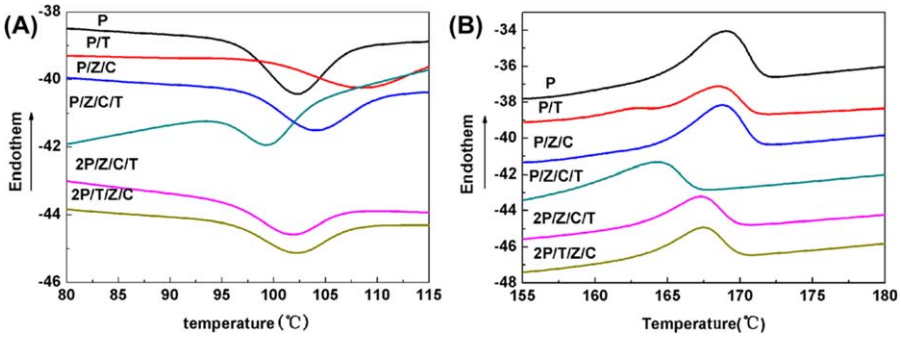

Figure 6. (A) T_c curves, (B) T_m curves of the samples of the P, P–T, and blends. [Color figure can be viewed in the online issue, which is available at wileyonlinelibrary.com.]

nearly 21% compared with PLA. This result was mainly attributed to the degradation of the composites caused by the ZnO, CCA, processing conditions, high temperature, and shear force during melt processing. ZnO initiated the breakdown of organic molecules by its photocatalytic ability. CCA accelerated the degradation of PLA and reduced its molecular weight by the hydrolysis of ester bonds. With the addition of TDI, the MFR values of the blends decreased by almost half, and the molecular weight increased by more than 6%. It was mainly because TDI retarded the degradation by the formation of high molecular chains.

Figure 5 shows the effects of TDI and different incorporation methods on the mechanical properties of the nanocomposites. PLA is a brittle and rigid polymer with a high tensile strength of 69.8 MPa and a very low strain at break of only 3%. It breaks without necking and shows brittle fracture; this was confirmed by the results of SEM micrographs.[16] The addition of TDI to the PLA matrix improved the molecular weight and led to an obvious increase in the bonding strength. This was in good agreement with previous studies,[28] which reported that the addition of methacryloyloxyethyl isocyanate improved the mechanical properties of PLA.

From the MFR results, we observed that the blends without TDI suffered adverse thermal degradation and mechanical degradation; this led to a sharp decrease in the mechanical properties with respect to the blends with TDI. After the addition of TDI to P–Z–C, marked increases in the tensile strength, strain at break, impact strength, and bending strength of 38.1, 33.8, 28.0, and 56.5%, respectively, were observed.

However, an increase in the agglomerated ZnO and worse interfacial interaction between the PLA matrix and ZnO were observed from TEM and SEM with respect to the blends without TDI. Najafi et al.[3] reported that the strain at break was sensitive to the dispersion of the blends, and the simultaneous incorporation of clay and Joncryl into the PLA matrix decreased the clay dispersion so that clay aggregates appeared. Taguet et al.[29] also observed that the elongation at break was directly linked to the state of the interface. Another study by Pongtanayut et al.[30] revealed that the elongate was greatly dependent on the dispersion and size distribution of the rubber particles in the PLA matrix. The strain at break of the blends with the incorporation of TDI and the masterbatches in batches was higher than that with the simultaneous incorporation by 67.0%. The incorporation in batches effectively decreased the ZnO agglomeration and increased the degree of uniform dispersion; this promoted the formation of a larger interfacial area and better interfacial interaction between the matrix and additives and led to an increase in the stress transfer from the PLA matrix to the inorganic phase and finally increased the tensile strength and bending strength.[31] The reduction in ZnO agglomeration also decreased the degree of interfacial debonding and craze density and led to an increase in the toughness.

Generally speaking, great increases in the tensile strength, strain at break, impact strength, and bending strength of 27.2, 67.0, 18.7, and 35.5%, respectively, were observed in the incorporation in batches compared with the simultaneous incorporation of the masterbatches and TDI.

Thermal Properties

DSC thermograms of the nanocomposites, obtained from the second heating run, are shown in Figure 6. The associated

Table IV. Thermal Parameters of the Samples

Sample	T_g (°C)	T_c (°C)	T_m (°C)	ΔH_m (J/g)	X_c (%)
PLA	65.0	102.2	169.0	18.9	20.2
PLA-TDI	66.8	108.9	168.6	14.4	15.5
PLA-Z-C	65.5	104.1	168.7	23.6	25.4
P-Z-C-T	67.0	102.1	167.2	24.0	25.8
2P-T-Z-C	67.4	101.7	167.3	20.1	21.6
2P-Z-C-T	67.1	100.4	167.4	20.7	22.3

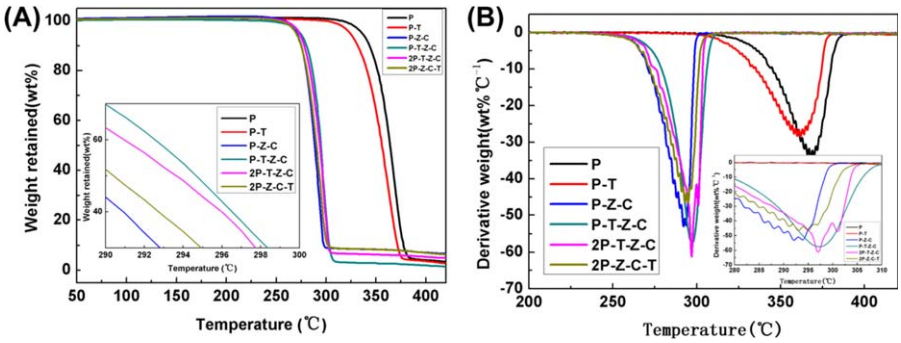

Figure 7. (A) Thermogravimetry and (B) DTG results of the P, P–T, and blends. [Color figure can be viewed in the online issue, which is available at wileyonlinelibrary.com.]

thermal parameters, such as the glass-transition temperature (T_g), cold crystallization temperature (T_c), melting temperature (T_m), melting enthalpy (ΔH_m), and degree of crystallinity (X_c), are summarized in Table IV. X_c was calculated on the basis of the ΔH_m value of 100% crystalline PLA being equal to 93 J/g.[19]

The pure PLA showed a clear glass transition at 65°C, whereas some significant changes were observed after the addition of TDI. It was noteworthy that T_g is a complex phenomenon that relies on several factors, such as intermolecular interactions, steric effects, chain flexibility, molecular weight, and the branching and crosslinking density.[32] In the case of the blends with TDI, the increase in T_g was mainly attributed to several aspects. On one hand, the restriction of the polymer chain mobility was introduced by the high molecular weight.[33] On the other hand, the hard groups of benzene in TDI in the polymer chains resulted in an increase in the chain stiffness.[11] Additionally, the ester group between ZnO and CCA and the reaction between PLA and TDI increased the interactions of the nanocomposites and thus led to the increment of T_g values.

After the addition of TDI to PLA, the cold crystallization was restrained as evidenced by an increase in T_c with a broad cold crystallization peak and a decrease in ΔH_m. It was noteworthy that the T_c of P–Z–C shifted to a lower temperature after the addition of TDI and the masterbatches in batches. This indicated that ZnO with less agglomeration and more interfacial areas had a marked heterogeneous nucleation effect on the PLA; this was in good agreement with previous studies that reported similar observations between the dispersion state of montmorillonite (MMT) and T_c.[27]

Table V. Parameters of the Thermogravimetry Curves of the P, P–T, and Blends

Sample	T_{onset} (°C)	$T_{5\%}$ (°C)	$T_{50\%}$ (°C)	T_D (°C)
P	316	337	365	369
P-T	300	325	356	361
P-Z-C	260	271	289	293
P-Z-C-T	235	270	294	300
2P-T-Z-C	257	274	294	301
2P-Z-C-T	253	271	291	295

The DSC results reveal that T_m remained unaltered with different incorporation methods of TDI and the masterbatches. This implied that TDI and the masterbatches had little influence on T_m. The increase in X_c after the addition of TDI and the masterbatches to PLA could have explained the heterogeneous nucleation effect of ZnO.

Dong[34] also reported a phenomenon in which a higher X_c of polymer composites let to better mechanical properties; this was consistent with the tensile or bending strengths of the blends after the addition of TDI.

The thermal stabilities of the samples measured by TGA and derivative TGA in a nitrogen atmosphere are presented in Figure 7. The characteristic thermal degradation temperatures, including the onset degradation temperature (T_{onset}), the temperatures of 5 and 50% mass loss ($T_{5\%}$ and $T_{50\%}$, respectively), and the temperature of the maximum rate of thermal degradation (T_D-from DTG), are summarized in Table V. All thermal degradation curves of the samples experienced a one-stage weight loss.

Jayaramudu et al.[35] reported that the thermal stability was mainly dependent on two controlling parameters, the molecular interaction between different macromolecules and some inherent characteristics of the components. In terms of P–T, the slight reduction in T_{onset} with respect to the neat PLA could be reasonably ascribed to the low thermal stability of the chain-extender decomposition products, for example, the carbamate, of which the thermal decomposition temperature was approximately 250°C.[36] Additionally, the volatilization might be delayed by the labyrinth effect of the large molecular chain structure with an increased entanglement density,[37] leading to a rapid decrease of T_D, which is in good agreement with the sample of 2P–Z–C–T. Although the sharp decrease of the decomposition temperature compared with P–T is mainly due to the degradation caused by CCA and ZnO and the thermal degradation during the process.

Yourdkhani et al.[38] reported that strong interfacial adhesion and effective dispersion provided a thermal barrier in the regions of the polymer and increased the thermal stability. Obvious increases in both T_{onset} and $T_{5\%}$ were observed with the incorporation in batches compared with the simultaneous incorporation; this indicated the incorporation in batches effectively

enhanced the compatibility between ZnO and PLA. This was confirmed by TEM micrographs and mechanical properties.

CONCLUSIONS

In this study, PLA/ZnO/CCA/TDI nanocomposites with perfect antibacterial activities and mechanical properties were prepared. TDI, basically as a chain extender, was introduced to the blends by different incorporation methods. The samples of TDI and the masterbatches incorporated in batches were found to effectively improve the compatibility and the homogeneous dispersion degree of ZnO in PLA matrix compared to disposable incorporation; thus, they exhibited more excellent mechanical properties, such as the strain at break and impact strength. Simultaneously, the addition of TDI retarded the degradation caused by CCA and ZnO and lead to an increased molecular weight; this improved the tensile strength and bending strength. The *R* of PLA/ZnO/CCA against *E. coli* was proven to 99.9%, whereas no remarkable reduction after the addition of TDI was observed. This indicated that the blends of PLA/ZnO/CCA/TDI had a strong antibacterial effect against *E. coli* over 99%.

ACKNOWLEDGMENTS

All of the authors listed this article contributed to it. The work was designed by Weihua Fan. The experiments were carried out by Yue Zhao. Aijing Zhang, Yukun Liu, Yanxia Cao, and Jinzhou Chen also offered a lot of help in the experiment. The article was written by Yue Zhao and finally modified by Weihua Fan.

REFERENCES

1. Krikorian, V.; Pochan, D. *J. Chem. Mater.* **2003**, *15*, 4317.
2. Baiardo, M.; Frisoni, G.; Scandola, M.; Rimelen, M.; Lips, D.; Ruffieux, K.; Wintermantel, E. *J. Appl. Polym. Sci.* **2003**, *90*, 1731.
3. Najafi, N.; Heuzey, M. C.; Carreau, P. *J. Compos. Sci. Technol.* **2012**, *72*, 608.
4. Jiang, L.; Zhang, J.; Wolcott, M, P. *Polymer* **2007**, *48*, 7632.
5. Pantani, R.; Gorrasi, G.; Vigliotta, G.; Murariu, M.; Dubois, P. *Eur. Polym. J.* **2013**, *49*, 3471.
6. Kairyte, K.; Kadys, A.; Luksiene, Z. *J. Photochem. Photobiol. B* **2013**, *128*, 78.
7. Torres, G. R.; Lindgren, T.; Lu, J.; Granqvist, C. G.; Lindquist, S. E. *J. Phys. Chem. B* **2004**, *108*, 5995.
8. Wu, Z.; Dong, F.; Zhao, W.; Guo, S. *J. Hazard. Mater.* **2008**, *157*, 57.
9. Hongqiao, Q.; Weiji, G.; Changshan, X. *J. Lumin.* **2008**, *29*, 591.
10. Zhao, W. D. S. Z. X.; Xiao-Zeng, L. Y. *Chin. J. Inorg. Chem.* **2007**, *23*, 1.
11. Ren, J.; Wang, Q. F.; Gu, S. Y.; Zhang, N. W.; Ren, T. B. *J. Appl. Polym. Sci.* **2006**, *99*, 1045.
12. Chen, B. K.; Shen, C. H.; Chen, S. C.; Chen, A. F. *Polymer* **2010**, *51*, 4667.
13. Kumar, A.; Pandey, A. K.; Singh, S. S.; Shanker, R.; Dhawan, A. *Free Radical Biol. Med.* **2011**, *51*, 1872.
14. Therias, S.; Larché, J. F.; Bussière, P. O.; Gardette, J. L.; Murariu, M.; Dubois, P. *Biomacromolecules* **2012**, *13*, 3283.
15. Kairyte, K.; Kadys, A.; Luksiene, Z. *J. Photochem. Photobiol. B* **2013**, *128*, 78.
16. Aijing, Z. M. S. Thesis, Zhengzhou University, **2014**.
17. Lipovsky, A.; Gedanken, A.; Lubart, R. *Photomed. Laser Surg.* **2013**, *31*, 526.
18. Di, W.; Zhen, S.; Zhao-Li, X.; Xiao, Z. Y. *Chin. J. Inorg. Chem.* **2007**, *23*, 1.
19. Murariu, M.; Doumbia, A.; Bonnaud, L.; Bonnaud, L.; Dechief, A. L.; Paint, M. F.; Campagne, C.; Devaux, E.; Dubois, P. *Biomacromolecules* **2011**, *12*, 1762.
20. He, Q.; Yuan, T.; Yan, X.; Ding, D.; Wang, Q.; Luo, Z.; Shen, T. D.; Wei, S.; Cao, D.; Guo, Z. *Macromol. Chem. Phys.* **2014**, *215*, 327.
21. Probst, N.; Madarasz, A.; Valkonen, A.; Papai, I.; Rissanen, K.; Neuvonen, A.; Pihko, P. M. *Angew. Chem. Int. Ed.* **2012**, *51*, 8495.
22. Balakrishnan, H.; Hassan, A.; Wahit, M. U.; Yussuf, A. A.; Razak, S. B. A. *Mater. Des.* **2010**, *31*, 3289.
23. Bitinis, N.; Verdejo, R.; Cassagnau, P.; Lopez-Manchado, M. A. *Mater. Chem. Phys.* **2011**, *129*, 823.
24. Gerard, T.; Budtova, T. *Eur. Polym. J.* **2012**, *48*, 1110.
25. Lin, S.; Guo, W.; Chen, C.; Ma, J.; Wang, B. *Mater. Des.* **2012**, *36*, 604.
26. Van, Den.; Oever, M. J. A.; Beck, B.; Müssig, J. *Compos. A* **2010**, *41*, 1628.
27. Zhang, N.; Zeng, C.; Wang, L.; Ren, J. *J. Polym. Environ.* **2013**, *21*, 286.
28. Chen, B. K.; Shih, C. C.; Chen, A. F. *Compos. A* **2012**, *43*, 2289.
29. Taguet, A.; Huneault, M. A.; Favis, B. D. *Polymer* **2009**, *50*, 5733.
30. Pongtanayut, K.; Thongpin, C.; Santawitee, O. *Energy Proc.* **2013**, *34*, 888.
31. He, Q.; Yuan, T.; Zhang, X.; Luo, Z.; Haldolaarachchige, N.; Sun, L.; Young, D. P.; Wei, S.; Guo, Z. *Macromolecules* **2013**, *46*, 2357.
32. Frone, A. N.; Berlioz, S.; Chailan, J. F.; Panaitescu, D. M. *Carbohydr. Polym.* **2013**, *91*, 377.
33. Ozkoc, G.; Kemaloglu, S. *J. Appl. Polym. Sci.* **2009**, *114*, 2481.
34. Dong, Y.; Ghataura, A.; Takagi, H.; Haroosh, H. J.; Nakagaito, A. N.; Lau, K. T. *Compos Part A-Appl S* **2014**, *63*, 76.
35. Jayaramudu, J.; Das, K.; Sonakshi, M.; Siva Mohan Reddy, G.; Aderibigbe, B.; Sadiku, R.; Sinha Ray, S. *Int. J. Biol. Macromol.* **2014**, *64*, 428.
36. Petersson, L.; Kvien, I.; Oksman, K. *Compos. Sci. Technol.* **2007**, *67*, 2535.
37. Mano, J. F.; Koniarova, D.; Reis, R. L. *J. Mater. Sci. Mater. Med.* **2003**, *14*, 127.
38. Yourdkhani, M.; Mousavand, T.; Chapleau, N.; Hubert, P. *Compos. Sci. Technol.* **2013**, *82*, 47.